Inorg. Chem. **2004**, *43*, 4988–4993

Synthesis, Structure, and Bonding of $BaAuTl_3$ and $BaAuIn_3$: Stabilization of $BaAl_4$-Type Examples of the Heavier Triels through Gold Substitution

Shengfeng Liu and John D. Corbett*

Ames Laboratory-DOE[1] and Department of Chemistry, Iowa State University, Ames, Iowa 50010

Received January 23, 2004

The title compounds have been synthesized by high temperature means and characterized by X-ray structural analysis, physical property measurements, and electronic structure calculations. The compounds crystallize in the three-dimensional tetragonal structure of $BaAl_4$, *I*4/*mmm*, $Z = 2$ ($a = 4.8107(4)$, 4.8604(2) Å, and $c = 11.980(2)$, 12.180(2) Å for $BaAuIn_3$ and $BaAuTl_3$, respectively). Gold randomly substitutes for 50% of the In or Tl in the apical (4*e*) positions in the network, generating apical–apical atom distances of 2.77 and 2.70 Å, respectively, values that are comparable to the single bond metallic radii sum for Au plus In, and 0.08 Å less than that for Au plus Tl. Relativistic effects appear to be important for both of the latter elements. The shrinkage in distances and increase in bond strengths evidently stabilize $BaAuTl_3$ relative to the distorted $BaTl_4$ with a presumably oversized triel lattice. EHTB band calculations indicate that the two compounds are electron-deficient relative to optimal Au–Tr and Au–Au bonding and metallic, the latter in agreement with measured properties of $BaAuTl_3$.

Introduction

Reduction of the triels (Tr), especially gallium, indium and thallium, by electropositive alkali or alkaline-earth metals customarily leads to unusual polar intermetallics that contain clusters or networks of the p-elements. Explorations on these polar intermetallic compounds in recent years have not only revealed a wealth of novel and peculiar structures but also expanded our chemical horizons into the nonclassical valence regime.[2−6] The results emphasize the greater complexity of these phases relative to classical valence (Zintl) compounds in which mainly the covalent bonding and hence electron counts govern structural stability. With alkaline-earth-metal cations, three-dimensional networks become more common, and factors beyond covalent bonding effects become competitive in structure determination, namely, the mutual optimization of the Madelung (site) energies and good space filling for cations encapsulated within the polyanionic network.[7−9]

We continue to explore ternary alkaline-earth-metal−transition metal−triel (Ae−T−Tr) systems in order to reveal and understand these situations better in the more versatile and diverse ternary systems. The relatively few reported indium-rich examples include $CaNiIn_4$, Ca_2CuIn_3,[10] and $CaTIn_2$ (T = Pd, Pt, Au),[11] which feature complex three-dimensional network structures. Our recently initiated explorations of analogous ternary thallium systems led to the discovery of (a) $SrPdTl_2$ and $SrPtTl_2$[12] isotypic with the above $CaTIn_2$ phases in the orthorhombic $MgCuAl_2$-type structure (stuffed $CaIn_2$) and (b) Ba_2AuTl_7[13] with a new 3D fused cluster structure. Size factors appear to be important in governing these structure selections as well. The last phase brings particular attention to the significant but rarely seen

* To whom correspondence should be addressed. E-mail: jcorbett@iastate.edu.

(1) This research was supported by the Office of the Basic Energy Sciences, Materials Sciences Division, U. S. Department of Energy (DOE). The Ames Laboratory is operated for DOE by Iowa State University under Contract No. W-7405-Eng-82.

(2) Nesper, R. *Angew. Chem., Int. Ed. Engl.* **1991**, *30*, 789.
(3) Belin, C. H E.; Tillard-Charbonnel, M. *Prog. Solid State Chem.* **1993**, *22*, 5.
(4) Corbett, J. D. In *Chemistry, Structure and bonding of Zintl Phases and Ions*; Kauzlarich, S. M., Ed.; VCH Publishers: New York, 1996; Chapter 4.
(5) Corbett, J. D. *Angew. Chem., Int. Ed.* **2000**, *39*, 670.
(6) Miller, G. J.; Lee, C.-S.; Choe, W. In *Inorganic Chenistry Highlights*; Meyer, G., Naumann, D., Wesemann, L., Eds.; Wiley-VCH Verlag-Gmbh: Weinheim, Germany, 2002; Chapter 2.
(7) Seo, D.-K.; Corbett, J. D. *J. Am. Chem. Soc.* **2000**, *122*, 9621.
(8) Seo, D.-K.; Corbett, J. D. *J. Am. Chem. Soc.* **2001**, *123*, 4512.
(9) Seo, D.-K.; Corbett, J. D. *J. Am. Chem. Soc.* **2002**, *124*, 415.
(10) Sysa, L. V.; Kalychak, Ya. M. *Crystallogr. Rep.* **1993**, *38*, 278.
(11) Hoffmann, R.-D.; Pöttgen, R.; Landrum, G. A.; Dronskowski, R.; Künen, B.; Kotzyba G. *Z. Anorg. Allg. Chem.* **1999**, *625*, 789.
(12) Liu, S.; Corbett, J. D. *Inorg. Chem.* **2003**, *42*, 4898.
(13) Liu, S.; Corbett, J. D. *Inorg. Chem.* **2004**, *43*, 2471.

10.1021/ic040010r CCC: $27.50
Published on Web 07/09/2004

differences regarding the bonding of these sixth period elements to one another for which relativistic effects and strong bonds appear to be particularly important.

A considerable family of triel phases with divalent cations exhibit the tetragonal $BaAl_4$-type and related structures, and they are of interest because of the robust structure and their electronic and bonding properties.[14−16] They are in fact stated[17] to be most populous of all crystal structure types, especially when all of the ternary examples are included. The binary examples of pertinence here are $AeAl_4$ and $AeGa_4$ which exist for Ae = Sr, Eu, Ba, and for $BaIn_4$,[18] all with the optimum 14 valence electrons per formula unit. The particular dependence of a still rather flexible structure type on atom sizes is illustrated by the fact that $SrIn_4$[7] as well as $EuIn_4$[19] with smaller cations exist in a distorted monoclinic structure with five-membered rather than six-membered rings. A different less distorted monoclinic structure occurs for $CaAl_4$[20] and $CaGa_4$,[21] for presumably related reasons. On the other hand, $BaTl_4$ evidently has an unknown structure,[22] probably because that cation is now undersized.

For completeness, we also note here that some analogous ternary compounds in the $BaAl_4$ family (with what is known as the $ThCr_2Si_2$ structure type) include $AeZn_2Ge_2$, A = Ca,[23] Sr.[24] There is also a 12-electron family of $CaZn_2Al_2$[25] and $AeCu_2Tt_2$, Ae = Ca, Sr and Tt = Si, Ge,[18] plus a series of nonstoichiometric, electron-richer $AeDi_{2-\delta}Tr_{2+\delta}$ for Ae = Ca, Sr, Ba; Di = Mg, Zn; Tr = Al, Ga.[16]

We here report the first examples of ternary alkaline-earth-metal compounds of In and Tl and the noteworthy effect that gold substitution has on stabilizing 12-electron $BaAuTl_3$ in the above $BaAl_4$ type structure when the analogous binary $BaTl_4$ has another structure. The latter effect appears to originate in part because of the smaller effective size presented on gold substitution for Tl, countering the well-known source of instability of this structure type with large Tr or small Ae noted above.[14−16] The relatively small size of gold (and lesser so for Tl) originates from well-known relativistic effects for 6th period elements in this region of the periodic table.[26] This give us the second opportunity to evaluate Au−Tl bonding between a pair of 6th period elements relative to the seemingly short 2.80 Å Au−Tl bonds which recently appeared in the report of the synthesis and new structure of Ba_2AuTl_7.[13] Reports of the substitution of Au (and other late transition metals) in $AeAl_4$ and $AeGa_4$ hosts have appeared,[27,28] but only in two cases has the limiting stoichiometry $AeAuTr_3$ been found, $SrAuAl_3$[29] according to powder data and $SrAu_{0.92(8)}Ga_{3.08(8)}$ by single crystal refinement.[30]

Experimental Section

Syntheses. All reactions were carried out in welded Ta tubes jacketed in a fused silica container utilizing the techniques described previously.[7−9] The elements used, Ba (99.9%), Au (99.95%), and In and Tl (99.999%), were all from Alfa-Aesar. All materials were handled in N_2- or He-filled gloveboxes with moisture levels below 0.1 ppm by volume. Before weighing, the surfaces of barium, indium, and thallium were cut clean with a scalpel.

Single crystals for $BaAuTl_3$ were first obtained during attempts to prepare a pure sample of a new ternary phase $Ba_3Au_{4-x}Tl_{7+x}$[22] that has the orthorhombic La_3Al_{11} structure type. Since a good value of x could not be established by X-ray diffraction means, a series of exploratory syntheses were carried out. Reaction of the trial composition $Ba_3Au_4Tl_7$ in a welded tantalum tube that was heated at 1050 °C for 4 h, quenched in water, then reheated at 600 °C for 7 days, and finally cooled at 5 °C/h to room temperature gave the first $BaAuTl_3$ crystals. An unknown phase was found from the loaded composition $BaAu_2Tl_2$ whereas the new phase Ba_2AuTl_7[13] was obtained from the composition $BaAu_{0.5}Tl_{3.5}$. The present $BaAuTl_3$ was subsequently obtained in high yield (>95%) from that loaded composition. Multiple EDX analyses on single crystals yielded the proportion $Ba_{1.00(4)}Au_{1.01(6)}Tl_{3.0(1)}$. After the structure of $BaAuTl_3$ had been established, single crystals of the isotypic $BaAuIn_3$ were produced in >95% yield from that loaded composition under the same reaction conditions. Attempted preparations of $SrAuTl_3$ and $SrAuIn_3$ gave only other phases and a gold-poorer example of the $BaAuTr_3$ structure, respectively.[31]

X-ray powder patterns for samples mounted between pieces of cellophane tape were collected with the aid of an Enraf-Nonius Guinier camera, Cu Kα radiation (λ = 1.540562 Å), and NIST silicon as an internal standard. Least-squares refinements of 21 and 22 lines for $BaAuTl_3$ and $BaAuIn_3$, respectively, indexed on the basis of the refined structural models resulted in the lattice constants given in Table 1. These generally more precise values were also used in distance calculations.

Structure Determination. Silvery block-shaped crystals of $BaAuTl_3$ were selected in the glovebox and sealed in thin-walled capillaries. The crystals were first checked by Laue photography to determine those most suitable for structural determinations. Diffraction data were collected on a Bruker APEX SMART CCD-equipped X-ray diffractometer at 23 °C with monochromated Mo Kα radiation. A total of 1315 frames were collected with an exposure time of 10 s/frame for each compound. The reflection intensities were integrated with the SAINT subprogram in the SMART software package.[32] The XPREP subprogram in the SHELXTL software package[33] was used for the space group determination, in which systematic absences indicated *I*4, *I*4/*m*, *I*4,

(14) Zheng, C.; Hoffmann, R. *Z. Naturforsch.* **1986**, *41B*, 292.
(15) Burdett, J. K.; Miller, G. J. *Chem. Mater.* **1990**, *2*, 12.
(16) Häussermann, U.; Amerioun, S.; Eriksson, L.; Lee, C.-S.; Miller, G. J. *J. Am. Chem. Soc.* **2002**, *124*, 4371.
(17) Pearson, W. B. *J. Solid State Chem.* **1985**, *56*, 278.
(18) Villars, P.; Calvert, L. D. *Person's Handbook of Crystallographic Data for Intermetallic Phases*, 2nd ed.; Americal Society of Metals: Metals Park, OH, 1991.
(19) Fornasini, M. L.; Cirafici, S. *Z. Kristallogr.* **1990**, *190*, 295.
(20) Zogg, H.; Schwellinger, P. *J. Mater. Sci.* **1979**, *14*, 1923.
(21) Bruzzone, G.; Fornasini, M. L.; Merlo, F. *J. Less-Common Met.* **1989**, *154*, 67.
(22) Liu, S.; Corbett, J. D. Unpublished results.
(23) Dörrscheidt, W.; Niess, N.; Schäfer, H. *Z. Naturforsch.* **1976**, *31B*, 890.
(24) Eisenman, B.; May, N.; Müller, W.; Schäfer, H.; Weiss, A.; Winter, J.; Ziegleder, G. *Z. Naturforsch.* **1970**, *5B*, 1350.
(25) Cordier, G.; Czech, E.; Schäfer, H. *Z. Naturforsch.* **1984**, *39B*, 1629.
(26) Pyykkö, P. *Chem. Rev.* **1988**, *88*, 63.
(27) Cordier, G.; Friedrich, T. *Z. Kristallogr.* **1992**, *201*, 306, 308.
(28) Grin, Yu.; Ellner, M.; Predel, B.; Cordier, G. *J. Alloys Compd.* **1994**, *216*, 207.
(29) Hulliger, F. *J. Alloys Compd.* **1995**, *216*, 207.
(30) Cordier, G.; Friedrich, T. *Z. Kristallogr.* **1992**, *201*, 310.
(31) The Sr−Au−In phase refined as *I*4/*mmm*, $SrAu_{0.47(1)}In_{3.53(1)}$, with z(M) = 0.3905(1), and a = 4.6712(7) Å, c = 12.357(3) Å from the diffractometer.[22]
(32) *SMART*; Bruker AXS, Inc.: Madison, WI, 1996.
(33) *SHELXTL*, version 5.1; Bruker AXS, Inc.: Madison, WI, 1998.

Table 1. Crystal Data and Structure Refinement for $BaAuIn_3$ and $BaAuTl_3$

	$BaAuIn_3$	$BaAuTl_3$
fw	678.8	947.4
space group, Z	$I4/mmm$ (No. 139), 2	$I4/mmm$ (No. 139), 2
unit cell dimensions[a] (Å, Å^3)		
a	4.8107(4)	4.8604(5)
c	11.980(2)	12.180(2)
V	277.25(2)	287.73(2)
d_{calcd} (Mg/m^3)	8.152	10.92
μ(Mo Kα) (mm^{-1})	45.59	59.85
final R indices[b]	0.0225, 0.0488	0.0322, 0.0698
R1, wR2 [$I > 2\sigma(I)$]		

[a] Refined from Guinier data with Si as internal standard, $\lambda = 1.540562$ Å, 23 °C. [b] $R1 = \sum||F_o| - |F_c||/\sum|F_o|$; $wR2 = [\sum w(|F_o|^2 - |F_c|^2)^2/\sum w(F^2_o)]^{1/2}$.

Table 2. Atomic Coordinates ($\times 10^4$) and Equivalent Isotropic Displacement Parameters (Å$^2 \times 10^3$) for $BaAuIn_3$ and $BaAuTl_3$

compd	atom	x	y	z	U(eq)[a]
$BaAuIn_3$	Ba	0	0	0	13(1)
	In	0	$^1/_2$	$^1/_4$	15(1)
	M[b]	0	0	0.3843(1)	18(1)
$BaAuTl_3$	Ba	0	0	0	12(1)
	Tl	0	$^1/_2$	$^1/_4$	15(1)
	M[c]	0	0	0.3890(1)	19(1)

[a] U(eq) is defined as one-third of the trace of the orthogonalized U_{ij} tensor. [b] M denotes 0.47(1) Au and 0.53(1) In, as refined. [c] M is 50:50 Au/Tl according to EDX and the $BaAuIn_3$ result.

Table 3. Important Bond Lengths [Å] in $BaAuIn_3$ and $BaAuTl_3$

$BaAuTl_3$		$BaAuIn_3$	
Tl−Tl × 4	3.4368(5)	In−In × 4	3.4017(5)
Tl-M × 4	2.9617(7)	In−M × 4	2.8941(6)
Tl−Ba × 4	3.8959(5)	In−Ba × 4	3.8413(5)
M−M	2.704(2)	M−M	2.7714(2)
M−T1 × 4	2.961(7)	M−In × 4	2.8941(6)
M−Ba × 4	3.8959(5)	Ba−In × 8	3.8413(5)
Ba−M × 8	3.6731(6)	Ba−M × 8	3.6731(6)

$I42m$, and $I4/mmm$ as possible space groups. The intensity statistics gave a clear indication of a centrosymmetric space group ($\langle E^2 - 1\rangle = 0.908$) for $BaAuTl_3$, but they were not very clear ($\langle E^2 - 1\rangle = 0.796$) for $BaAuIn_3$. However, the centric space group $I4/mmm$ gave the most satisfactory refinements of both. Application of direct methods in SHELXTL in the latter case revealed all of the In, mixed (Au + In), and Ba atoms. The mixed site for In + Au refined to 0.53(1) In, 0.47(1) Au, whereas that with Tl + Au was set at 50:50 according to the synthetic results, the EDX analyses (above), the In precedent, and bonding expectations (see Results and Discussion section). The full-matrix least-squares refinement converged at $R(F) = 3.27\%$, $wR2 = 7.08\%$, and GOF = 1.086 for $BaAuTl_3$ and $R(F) = 2.25\%$, $wR2 = 4.88\%$, and GOF = 1.243 for $BaAuIn_3$. The largest residual peak and hole in the ΔF maps were 4.50 and −2.26 e/Å^{-3} for $BaAuTl_3$ and 1.84 and −1.92 e/Å^{-3} for $BaAuIn_3$. Some aspects of the data collection and refinement are listed in Table 1. Table 2 gives the atomic positional and isotropic equivalent displacement parameters, and Table 3 lists important interatomic distances in the two structures calculated with the aid of the Guinier-based lattice constants. More detailed crystallographic information as well as the anisotropic displacement parameters are available in the Supporting Information.

Properties. Electrical resistivities of the $BaAuTl_3$ phase were measured at 4 MHz over 110−251 K by the electrodeless "Q" method with the aid of Hewlett-Packard 4342 A Q meter.[34] For this purpose, 86.1 mg of a powdered sample with grain diameters between 150 and 250 μm was dispersed with chromatographic alumina and sealed under He in a Pyrex tube. Magnetic susceptibility measurements were carried out at 3 T over 8−350 K on a Quantum Design (MPMS) SQUID magnetometer, principally to distinguish between diamagnetic and Pauli-paramagnetic characteristics. A 101.9 mg quantity of powdered $BaAuTl_3$ was held between the faces of two fused silica rods that were in turn fixed and sealed inside an outer silica tube. M versus H data checked at 5 K showed the absence of significant magnetic impurities.

EHTB Calculations. All the extended Hückel tight binding band calculations were carried out using the CAESAR program developed by Whangbo and co-workers.[35] The data utilized for EHTB band calculations were as follows: Ba, 6s −5.49, 1.21; 6p −3.56, 1.21;[7] Tl, 6s −11.6, 2.52; 6p −5.8, 1.77;[36] In, 5s −12.6, 1.903; 5p −6.19, 1.677;[37] Au, 6s −10.92, 2.602; 6p −5.55, 2.584; 5d −15.076, 6.163, 0.6851, 2.794, 0.5696;[38] M (averages) (Au + In), 6s −11.76, 2.25; 6p −5.87, 2.130; M (Au + Tl), 6s −11.26, 2.56; 6p −5.68, 2.18. The Au 5d orbitals were not included in later calculations after it was discovered that these fell in a narrow band around −14 eV.

There are still uncertainties as to the best parameters for these calculations. One is the question whether the Tl energy and orbital parameters are suitably lowered and contracted in a relativistic sense compared with those for gold. Also, substantial charge appears to pass from Ba of course and from thallium (or indium) to gold as well. Charge iteration of the energies of Tl versus Sb p orbitals in a related but ordered polar case Na_6TlSb_4 produced a decrease of −3.5 eV in the Tl 6p energy because of charge transfer to Sb.[39] The problem here is further complicated by the 50:50 mixture of Au and Tl or In present on the M site for which we have used just the average of the parameters for the pairs of atoms involved. However, tight binding[13] versus relativistic[40] LMTO calculations on Ba_2AuTl_7 do give some general credence to the former results except that the Au 6s orbital energy is too high and the Au 5d energies and participation in the bonding are both too low.

Results and Discussion

Structure. The two new isostructural compounds $BaAuTl_3$ and $BaAuIn_3$ are the first ternary examples of the bct parent structure $BaAl_4$ ($I4/mmm$) for the heavier triels. The well-known structure type can be described in terms of a three-dimensional $[AuTr_3^{2-}]$ polyanion network in which barium atoms at the center and corners of the cell fill Tr, Au polyhedra in a 3D network, as shown in Figure 1. The structure type can be viewed as a condensed version of the PbO structure, a square basal net of Pb with apical O atoms capping squares on alternate sides, except that these nets are now condensed side-by-side at pairs of former oxygen apex sites into a 3D network. The square net here consists of Tl or In atoms with the interconnected apical sites essentially 50:50 Tr/Au or In/Au, hereafter designated as M.

(34) Zhao, J. T.; Corbett, J. D. *Inorg. Chem.* **1995**, *34*, 378.
(35) Ren, J.; Liang, W.; Whangbo, M.-H. *CAESAR for Windows*; Prime-Color Software, Inc.: North Carolina State University: Raleigh, NC, 1998.
(36) Whitmire, K. H.; Ryan, R. R.; Wasserman, H. J.; Albright, T. A.; Kang, S. K. *J. Am. Chem. Soc.* **1986**, *108*, 6831. (b) Janiak, C.; Hoffmann, R. J. *J. Am. Chem. Soc.* **1990**, *112*, 5924.
(37) Hinze, J.; Jaffé, H. H. *J. Chem. Phys.* **1963**, *67*, 1501.
(38) Komiya, S.; Albright T. A.; Hoffmann, R.; Kochi, J. K. *J. Am. Chem. Soc.* **1977**, *99*, 8440.
(39) Li, B.; Chi, L., Corbett, J. D. *Inorg. Chem.* **2003**, *42*, 3036.
(40) Miller, G. J.; Corbett, J. D. Unpublished results.

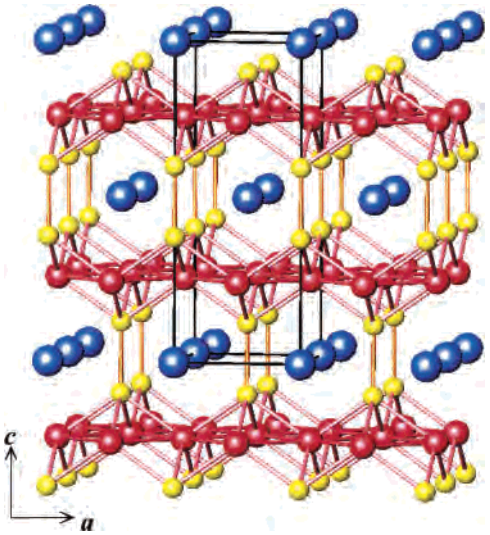

Figure 1. [100] view of the crystal structure of $BaAuTl_3$. The Ba, Tl, and M (Tl + Au) atoms are colored blue, red, and yellow, respectively.

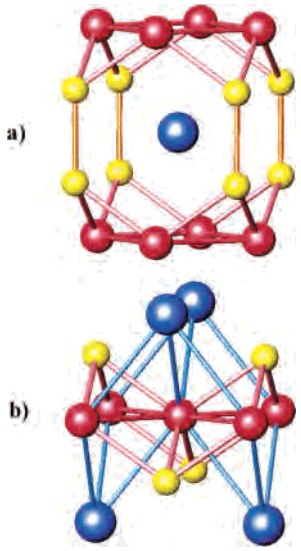

Figure 2. (a) The polyanion atoms around each barium atom and (b) the environment of Tl in $BaAuTl_3$. The Ba, Tl, and M (Tl + Au) atoms are colored blue, red, and yellow, respectively.

The effective coordination polyhedron for Ba atoms corresponds to a 16-atom figure defined by separate rectangular blocks of 8 Tr and 8 M, as shown in Figure 2a. The 8 M sites are distinctly closer to Ba in the new phases. Each basal triel atom Tr_b is surrounded by four other coplanar basal atoms, nearly tetrahedrally by four apical M atoms, and four Ba neighbors, Figure 2b. Each M atom is in turn surrounded by four basal triel atoms and one apical M atom in a square pyramidal manner, plus the four Ba neighbors. The capped square nets $^2_\infty[Tr_{4/4}M]$ in the $a-b$ plane can also be reconstituted as perpendicular square pyramidal units interjoined by M−M bonds.[15]

A number of the distances in these compounds are noteworthy, Table 3. A selection of these for the present and some related $BaTr_4$ members and some reference distances are collected in Table 4. Two points need to be recalled: (1) $BaAl_4$-type structures are good candidates for matrix effects (the cage dimensions respond appreciably to the size of the encapsulated cation[16]), and (2) Au is well-known for substantial relativistic contractions of its s and p orbital sizes and decreases of the energies of both, especially the 6s orbitals.[26] One measure of the former, the single bond metallic distance for Au deduced from the metal by Pauling,[42] 2.679 Å, is distinctly less than that for In, 2.842 Å, as well as for Tl (2.874 Å). The Ga value is 2.492 Å. The increase of only 0.03 Å from In to Tl values reflects a relativistic contraction for the latter as well.

Table 4. Bond Distances in Some $BaAl_4$-Type Phases (Å)

compd	Tr−Tr	Tr−M	M−M	(∑(PSB)[a])	Ba−M	*c*/*a*	*V* (Å^3)
$BaGa_4$[b]	3.23	2.68[d]	2.59	(2.49)	3.47	2.36	224
$BaIn_4$[c]	3.49	2.92[d]	2.81	(2.84)	3.76	2.41	289
$BaAuIn_3$	3.40	2.89	2.77	(2.76)	3.67	2.490	277
$BaAuTl_3$	3.44	2.96	2.70	(2.78)	3.69	2.506	288

[a] Pauling single bond radii sum, Tr−Tr or Au−Tr. [b] Ref 16. [c] Ref 41 (powder refinement). [d] M = Tr_{apical}.

The Tr−Tr distances in the basal plane are in any case not particularly unusual, being 0.5−0.6 Å longer than the single bond reference values. These interactions have generally been considered as nonbonding in two extensive analyses of $BaAl_4$-type materials,[14,15] instead affording some flexibility in adjusting the $a-b$ framework to cation size. According to earlier considerations, the bonding elsewhere in the structure can be simplified as a 5-center−6-electron delocalized bonding scheme within two $(Tr_b)_4Tr_a$ square pyramids and more classical 2-electron−2 center Tr_a-Tr_a bond between them for a total of 14 electrons. In many of the known cases, the differences between $d(Tr_b-Tr_a)$ and $d(Tr_a-Tr_a)$ are small and often slightly negative, whereas this difference is increasingly positive for 12e$^-$ members.[15] $BaIn_4$ also falls in the latter class dimensionally. The apical position is recognized as that with the most negative relative population (see below), and the (partial) substitution of gold there and shorter Ba distances thereto are as expected. The two bonding distances Tr_b-Tr_b and Tr_a-Tr_a (M−M) show decreases of 0.03−0.04 Å on conversion of $BaIn_4$ to $BaAuIn_3$, which also involves a reduction from 14 to 12 electrons per formula unit. The lattice dimensions *a*, *c*, *V* decrease on insertion of 50% of the smaller Au on the In_a site with a noticeable increase in *c*/*a*; i.e., the *c* components of the shrinkage in *d*(In−M) and an *d*(M−M) are less than in basal *d*(In−In), largely following a −0.09 Å decrease in *d*(Ba−M). (Recall that all of the $BaIn_4$ data come from a powder refinement, so these values are probably not highly accurate.)

Although $BaTl_4$ is unknown in this structure, the smaller Au atom enables what cannot be accomplished by Tl alone and evidently gives stronger bonding as well. The Tr−M distance logically increases 0.07 Å on then going from $BaAuIn_3$ to $BaAuTl_3$, but the M−M distances actually decrease a similar amount, again[13] appearing to reflect on the remarkable strength and the shortness of the Tl−Tl, Tl−

(41) Bruzzone, G. *Acta Crystallogr.* **1965**, *18*, 1081.
(42) Pauling, L. *Nature of the Chemical Bond*, 3rd ed.; Cornell University Press: Ithaca, NY, 1960; p 403.

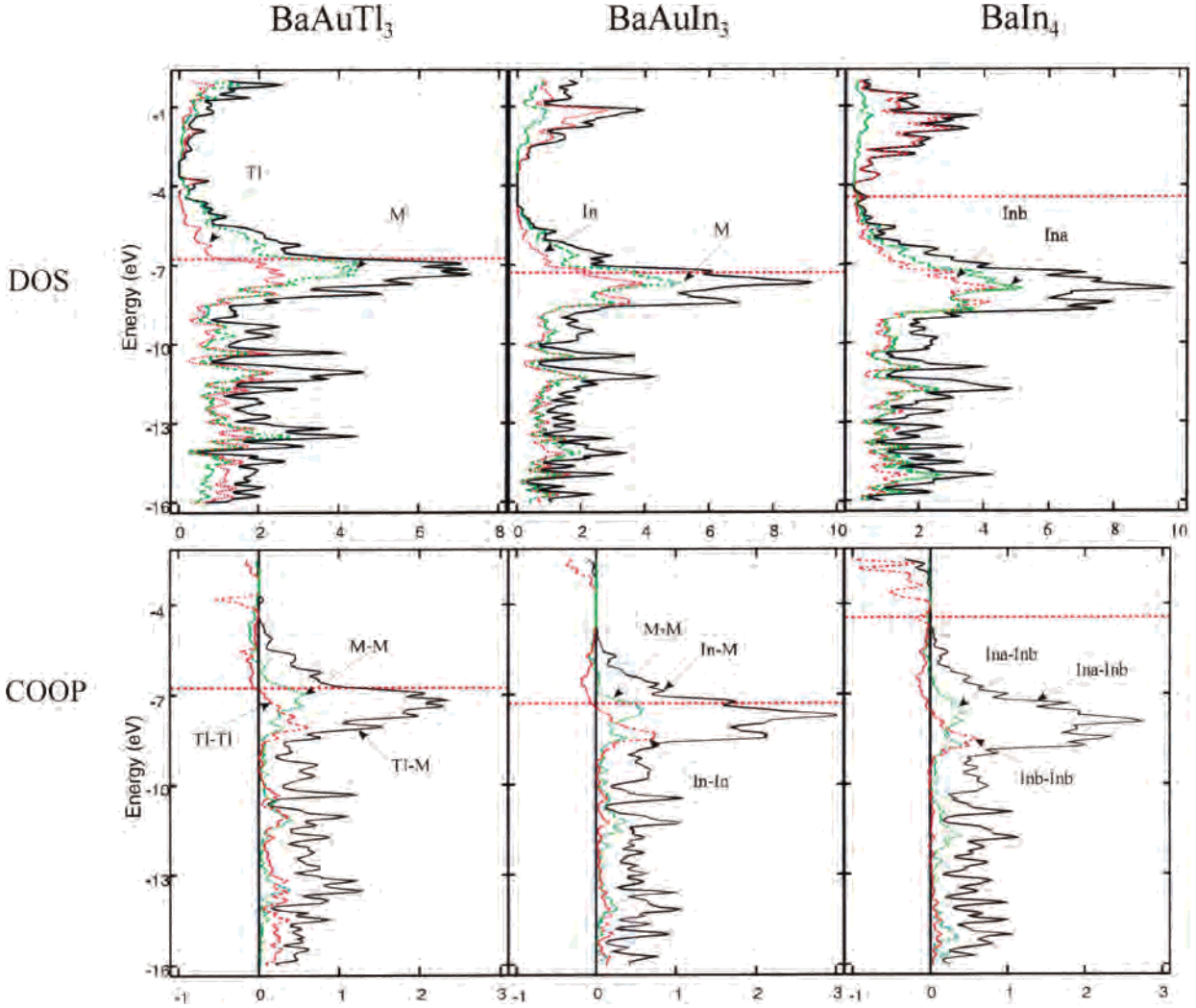

Figure 3. Densities-of-states (DOS) (top) and COOP data (bottom) for, left to right, $BaAuTl_3$, BaAuIn, and $BaIn_4$. The black, red, and green lines refer to total DOS and the PDOS of basal In or Tl and of the apical In or M (In + Au or Tl + Au) site, respectively. In the COOP data, the solid line denotes basal−apical interactions (Tr−M or In−In), the red, basal−basal, and the green, apex−apex bonding.

Au, and Au−Au components of the mixed M−M bonding. The M−M distances for the three In and Tl examples listed are all less than the reference sum of the Pauling single bond values, and d(M−M) in $BaAuTl_3$ is by most standards very short at 2.704(2) Å. For comparison, the shortest d(Au−Tl) about 5-bonded Au in Ba_2AuTl_7 is 2.80 Å. The overlap populations will be seen to follow the bond lengths trends relatively well, too (below).

Broad considerations of the variety of binary and ternary $BaAl_4$-type examples make it clear that variations in the c axis and, especially, the apical−apical bonds are the main means by which these compounds adjust to cation size.[16] The barium cation seems well matched to the In_4^{2-}, $AuIn_3^{2-}$, and $AuTl_3^{2-}$ nets in that such short and evidently strong apex−apex (M−M) bonds are attained, Table 4. The same feature has been noted for Al_a-Al_a and Ga_a-Ga_a bonds in their calcium salts.[16] Another important feature of the gold derivatives is the unevaluated gain in Madelung energy associated with the greater electronegativity of gold. Electronics probably preclude achievement of the ever better $BaAu_2Tl_2$ (10 electrons), but $BaHg_2Tl_2$ might be a worthy target.

Chemical Bonding and Electronic Structure. Heretofore, the electron-poorer 12-electron systems with $BaAl_4$ structures have been largely limited to $SrAuTr_3$, Tr = Al, Ga, $CaZn_2Al_2$, and $Ae_2Cu_2(Tt)_2$, Tt = Si, Ge, plus off-stoichiometry and electron-richer 1:2 − δ:2 + δ examples with Ca−Ba, Mg, or Zn, and Al or Ga, respectively. Inclusion of 50% gold in apical sites now provides In and Tl members of the $12e^-$ group as well.

The electronic band structures were calculated for the complete structure of $BaAuIn_3$ and $BaAuTl_3$ as well as for $BaIn_4$ with the aid of the extended Hückel tight-binding (EHTB) method. The total and projected partial densities-of-states (DOS) for Tr_a and Tr_b and the crystal orbital overlap populations (COOP) for Tr−Tr (basal), Tr−M, and M−M are given in Figure 3 for, left to right, $BaAuTl_3$, $BaAuIn_3$, and $BaIn_4$. A total of 24, 24, and 28 valence electrons per cell (Z = 2) fill the orbitals up to the Fermi energies of −7.30, −6.86, and −4.44 eV, respectively. The DOS curves of the three compounds are very similar except that E_F naturally falls higher and at a pseudogap for $BaIn_4$, and the valence band for that phase is distinctly broader. (Parameters for the M sites in the ternaries utilized an average of the

Table 5. MOP Values for the Various Bonds in $BaGa_4$, $BaIn_4$, $BaAuIn_3$, and $BaAuTl_3$

compd	bond[a] (Å)	MOP
$BaGa_4$	Ga_a-Ga_a (2.59)	0.79
	Ga_a-Ga_b (2.68)	0.59
	Ga_b-Ga_b (3.23)	0.075
$BaIn_4$	In_a-In_a (2.81)	0.80
	In_a-In_b (2.92)	0.59
	In_b-In_b (3.49)	0.10
$BaAuIn_3$	M−M (2.77)	0.69
	M−In (2.89)	0.49
	In−In (3.40)	0.18
$BaAuTl_3$	M−M (2.70)	0.69
	M−Tl (2.96)	0.46
	Tl−Tl (3.44)	0.22

[a] $BaTr_4$ distance data from ref 41.

data for Tr and Au.) The incomplete filling of the bonding bands seen for the gold salts and the unoptimized M−M COOP functions are of course presumably compensated by the gain in Madelung energies.

Judging from the COOP curves (and neglecting the differences in overlap integrals), the Tr_b-M (In_b-In_a) contributions are largest, whereas the basal−basal and apical−apical data are lower and about comparable in the lower and upper parts of the valence band, respectively. The basal−basal bonding is optimized in the ternaries but not the M−M interactions, whereas both are substantially optimized for $BaIn_4$. More pertinent and useful are the Mulliken overlap populations for the three bond types in the three phases along with similar data for $BaGa_4$ that are listed in Table 5. The dominant values (and presumably strengths) of the apical−apical bonds are striking (0.69−0.80), and the apical−basal effects are also substantial.

The closest network atoms about the Ba cations are the apical sites (M), Table 4, consistent with their greater (neutral atom) negativity.[43] With only Tl present at this site in $BaTl_4$, all we know for sure is that other phases would be more stable, presumably because Tl is too large. The contraction when 50% gold is included in M and the stronger bonds are sufficient to stabilize this structure type. In an MO description, the four electrons removed per cell on transition to the gold products come from π^* states on M.[15]

Physical Properties. The measured resisitivities of $BaAuTl_3$ shown in Figure 4 increase linearly with temperature. The isotropic room temperature value is about 34.1 $\mu\Omega\cdot$cm, with a mean temperature dependence of 0.10% K^{-1}. The linear increase indicates that $BaAuTl_3$ is a fairly normal metal

(43) The Mulliken electronegativities for In, Tl, and Au are 3.1, 3.2, and 5.78 eV, respectively: Pearson, R. G. *Inorg. Chem.* **1988**, *27*, 734.

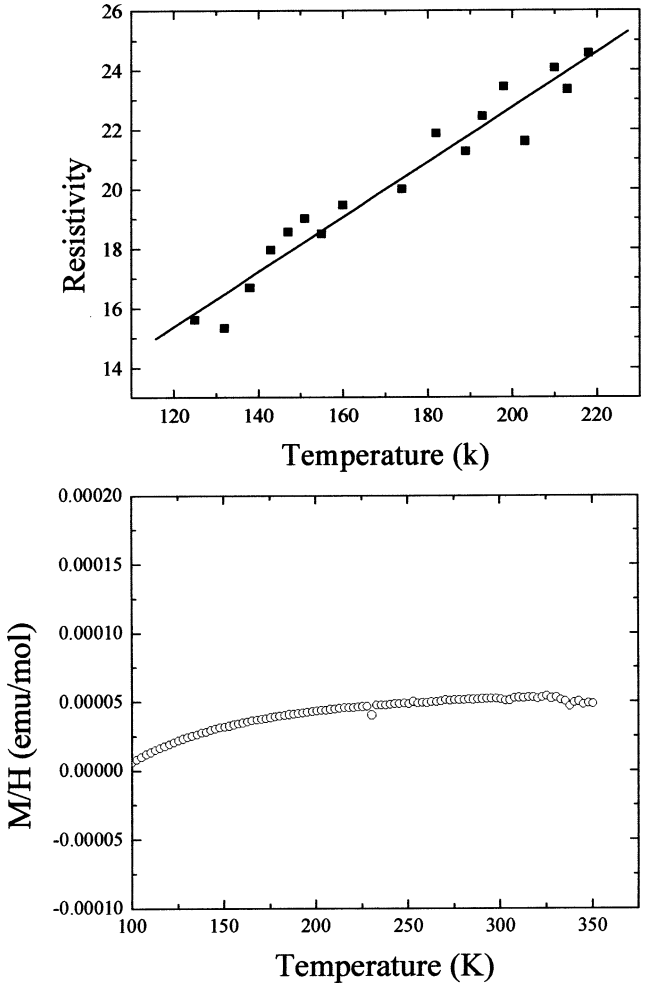

Figure 4. Resistivities (top) and molar magnetic susceptibilities (bottom) as a function of temperature (K) for $BaAuTl_3$.

in the temperature range of the measurement. Magnetic susceptibilities of $BaAuTl_3$ also given in Figure 4 are small, and the compound is essentially Pauli-paramagnetic with $\chi_m = 5.03 \times 10^{-5}$ emu/mol above −200 K. Both properties are in agreement with theoretical expectations.

Acknowledgment. We are indebted to S. Budko for the magnetic susceptibility data.

Note Added in Proof: The structure of $BaTl_4$ has been established to be of the EuI_4 type, J.-C. Dai and J. D. Corbett.

Supporting Information Available: Additional crystallographic information for $BaAuTl_3$ and $BaAuIn_3$. This material is available free of charge via the Internet at http://pubs.acs.org.

IC040010R